Journal of Applied Electrochemistry (2005) 35:741–750
DOI 10.1007/s10800-005-1385-5

Photoelectrocatalytic degradation of bisphenol A in aqueous solution using a Au–TiO_2/ITO film

X.Z. LI[1,*], C. HE[1], NIGEL GRAHAM[1] and Y. XIONG[2]
[1]*Department of Civil and Structural Engineering, The Hong Kong Polytechnic University, Hong Kong, China*
[2]*School of Chemistry and Chemical Engineering, Sun Yat sen University, Guangzhou 510275, China*
*(*author for correspondence, e-mail: cexzli@polyu.edu.hk; fax: +852-2334-6389)*

Received 4 January 2005; accepted in revised form 5 January 2005

Key words: Au, bisphenol A, EDCs, photoelectrocatalysis, photoelectrochemistry, TiO_2

Abstract

A series of Au–TiO_2/ITO films with nanocrystaline structure was prepared by a procedure of photo-deposition and subsequent dip-coating. The Au–TiO_2/ITO films were characterized by X-ray diffraction, scanning electronic microscopy, electron diffraction, X-ray photoelectron spectroscopy, and UV–VIS diffuse reflectance spectroscopy to examine the surface structure, chemical composition, the chemical state of metal, and the light absorption properties. The photocatalytic activity of the Au–TiO_2/ITO films was evaluated in the photocatalytic (PC) and photoelectrocatalytic (PEC) degradation of bisphenol A (BPA) in aqueous solution. Compared with a TiO_2/ITO film, the degree of BPA degradation using the Au–TiO_2/ITO films was significantly higher in both the PC and PEC processes. The enhancement is attributed to the action of Au deposits on the TiO_2 surface, which play a key role by attracting conduction band photoelectrons. In the PEC process, the anodic bias externally applied on the illuminated Au–TiO_2/ITO film can further drive away the accumulated photoelectrons from the metal deposits and promote a process of interfacial charge transfer.

1. Introduction

The presence of endocrine disrupting chemicals (EDCs) in the environment and, specifically in municipal and industrial wastewaters, is of growing concern. Chemicals such as bisphenols, dioxins, pesticides, phthalates, alkylphenolic compounds, furans, synthetic steroids, and some natural compounds, have been shown to have the potential to interfere with the endocrine systems of a wide range of living organisms, including humans, in various ways to cause an adverse response or disruption to their health, growth, and reproduction [1–5]. Most of these EDCs can not be removed completely from wastewaters by conventional biological treatment, such as by activated sludge processes [6, 7], which leads to their presence in receiving waters where they have the potential to adversely affect human and animal life even at very low concentrations [5, 8]. Consequently, advanced treatment technologies are required to effectively eliminate these pollutants in drinking water sources and wastewater effluents.

In recent years, the process of heterogeneous photocatalysis, especially with the use of TiO_2 as a catalyst, has been extensively studied in the purification of water and wastewater. This is because almost all organic pollutants, including those toxic at low concentration, can be decomposed to carbon dioxide with the strong oxidizing power of the photogenerated holes of TiO_2 [9–11]. However, this technique is insufficient for practical application due to the rapid recombination of active electrons and holes after photoexcitation [12, 13]. To further improve the efficiency of photocatalytic (PC) oxidation reactions, the TiO_2 catalyst can be modified by the addition of various impurities. For example, different metals or metallic oxides can be added either into the TiO_2 structure by doping, implanting or coprecipitating or onto the TiO_2 surface by coating or photodepositing as metal islands [12, 14–22]. Among these methods, one approach is the deposition of precious metals such as Au and Pt on the surface of the TiO_2 catalyst through a photoreduction reaction. A study by Bamwenda et al. [14] found that the presence of deposited Au on the surface of TiO_2 could significantly improve its photocatalytic activity and achieved the best photocatalytic efficiency with 1.0 wt% Au.

The development of photoelectrocatalytic (PEC) oxidation processes with an externally-applied anodic bias has also been receiving attention in recent years [13, 23–26]. So far, most studies have been related either to the PC processes with the metal-loaded TiO_2 powders or

to the PEC processes with ordinary TiO_2 films [13, 23–26]. More recently, a few studies have focused on the PEC reaction using metal-loaded TiO_2 films, in which TiO_2 powder was first coated on an electrode material such as a glass plate and then metals were deposited by photoreduction [21, 22, 27–30]. In our previous studies, some metal-loaded TiO_2 films including Pt–TiO_2/Ti [21], Ag–TiO_2/ITO [27, 28, 29], and Cu–TiO_2/ITO [30] were investigated by applying an external anodic bias. These studies determined that the optimum contents of Ag and Cu on the TiO_2 films were approximately 1 and 1.5%, respectively, and also found that higher metal loading resulted in a decrease in photocatalytic activity due to two reasons: (1) the high coverage of TiO_2 film surface by metal deposits eliminates the efficiency of light absorption by the catalysts [31]; and (2) the cluster or aggregation of metal deposits on the TiO_2 surface changes the function from an electron separation center to an electron recombination center, and consequently reduces the photocatalytic activity [32]. However, if the amount of metal deposition is well below its optimum dosage, the metal-loaded TiO_2 has no significant difference to a pure TiO_2 catalyst. Therefore, a good catalyst with high photocatalytic activity should have a certain amount of metal deposition but with low coverage of the TiO_2 surface and should also avoid clustering or aggregation of metal deposits on the TiO_2 catalysts.

In this study, Au was uniformly deposited on the surface of TiO_2 powder by photoreduction in a TiO_2 suspension. Then the Au–TiO_2 powder was coated on an indium–tin oxide (ITO) plate by a dip-coating method. The photocatalytic activity of the Au–TiO_2/ITO films was evaluated in the PC and PEC processes by measuring the degradation of bisphenol A (BPA). BPA was chosen a model EDC in aqueous solution since it is a synthetic chemical produced worldwide in millions of tons each year and is used to manufacture polycarbonate and epoxy resins, which are used in baby bottles, as protective coatings on food containers [33, 34], and for composites and sealants in dentistry [35]; it is a suspected endocrine disrupting compound.

2. Experimental

2.1. *Materials*

TiO_2 (Degussa P25) powder with an average particle size of 30 nm and surface area of 50 $m^2\ g^{-1}$ was purchased from Degussa AG Company as a regular TiO_2 catalyst. BPA (2, 2-bis(4-hydroxyphenyl)propane) chemical (>99% purity) was purchased from Aldrich Chemical Company and its molecular structure is shown in Figure 1. The indium-tin oxide (ITO) conductive glass plates with a thickness of 1.3 mm were obtained from Shenzhen Nanya Technology Ltd., China. Other chemicals at analytical grade were obtained as reagents and used without further purification. Deionized distilled water was used throughout the experiments.

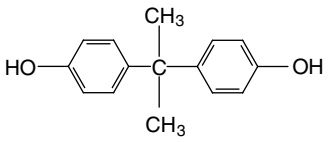

Fig. 1. Molecular structure of bisphenol A.

2.2. *Preparation of TiO_2/ITO and Au–TiO_2/ITO films*

A TiO_2/ITO film was first prepared according to the procedure described in the literature [23]. 40 g of TiO_2 powder was added to 500 ml of distilled water. The TiO_2 slurry was sonicated for 30 min to break up loosely-attached aggregates and then vigorously agitated to form a fine TiO_2 suspension. The TiO_2 in the suspension was loaded onto the ITO glass plate (1.0 cm × 5.0 cm) by a dip-coating, drying and sintering procedure. The TiO_2-coated ITO film was dried for 15 min on a hot plate at 100 °C and subsequently sintered in a muffle furnace at 400 °C for 2 h to obtain the TiO_2/ITO film. The quantity of TiO_2 loading was about 1.07–1.10 mg cm^{-2}.

An Au–TiO_2/ITO film was prepared by photo-depositing Au on TiO_2 particles and then loading the Au–TiO_2 powder onto the ITO conductive glass plate. The preparation procedure was described as follows: 8 g of TiO_2 powder was added into 100 ml of Au precursor solution containing 10 mmol l^{-1} $HAuCl_4$ and HCOOH; the mixture was vigorously agitated for 1 h to form a fine TiO_2 suspension after sonication for 30 min; then the suspension was illuminated with a 500-W high-pressure mercury lamp for 2 h to conduct the photoreduction reaction, in which Au^{3+} was reduced to Au and uniformly deposited on the TiO_2 particles; these Au-loaded TiO_2 particles were then coated onto the ITO glass plate by the same dip-coating, drying and sintering procedure to eventually obtain the Au–TiO_2/ITO film. A series of Au–TiO_2/ITO films was prepared with a Au content of 0.5, 1.0, 1.5, and 2.0% (wtAu/wtTiO_2), respectively, by changing the amount of $HAuCl_4$ in the Au precursor solution. An EDS analysis was carried out to confirm the amount of the Au deposition in the TiO_2/ITO films. The results indicated that the amount of Au in these four Au–TiO_2/ITO films prepared by the photoreaction were 0.63, 1.1, 1.57, and 2.07% (Wt. Au/Wt. TiO_2), corresponding to the samples with a nominal Au content of 0.5, 1.0, 1.5, and 2.0% (Wt. Au/Wt. TiO_2), respectively.

2.3. *Characterization of TiO_2/ITO and Au–TiO_2/ITO films*

The prepared TiO_2/ITO and Au–TiO_2/ITO films were first examined by spectrophotometry (Shimaszu UV-PC3101PC) with an integrating sphere (Specular Reflectance ATT.5DEG) to record their diffuse reflectance spectra (DRS), in which the baseline was corrected by using a calibrated sample of barium sulfate. Both the

TiO_2/ITO and Au–TiO_2/ITO films were then examined by scanning electron microscopy (SEM) with a secondary electrons detector (Leica, Stereoscan 440). Energy dispersive spectroscopy (EDS) was also obtained through the SEM equipped with a link analyzer (Oxford, ISIS-300) to determine the amount of Au deposition in the Au–TiO_2/ITO films. The films were further analyzed by X-ray diffraction (XRD) using a diffractometer (Philips, Xpert system) with radiation of a Cu target (K_α, $\lambda = 0.15406$ nm). X-ray photoelectron spectroscopy (XPS) of the prepared films was recorded with the PHI Quantum ESCA microprobe system using the MgK_α line of a 250-W Mg X–ray tube as a radiator. The fitting of XPS curves was obtained with the Multipak 6.0A software.

2.4. *Experiments of PC and PEC oxidation*

Aqueous BPA solution was prepared by dissolving BPA into distilled water, in which 0.05 mol l^{-1} Na_2SO_4 was also added as supporting electrolyte. Both the PC and PEC oxidation reactions were carried out in a photoreactor system as shown in Figure 2, consisting of two chambers (A and B, 2.0 cm × 1.1 cm × 8.0 cm) connected via a salt bridge. The PC reaction was conducted using chamber A only, and the PEC reaction was performed using both chambers. An 8-W UV lamp with a peak emission at 365 nm was used as a UV source and air bubbling was continuously provided. Either the TiO_2/ITO or Au–TiO_2/ITO plate was placed in chamber A and used as the anode, while a Pt electrode and a saturated calomel electrode (SCE) were positioned in chamber B and used as counter and reference electrodes, respectively. About 10 ml of aqueous BPA solution was used in both the PC and PEC reactions and the pH of the solution was not controlled during the reaction. The photoelectrochemical measurement was performed with a potentiostat (Model CH 650, Shanghai).

2.5. *Analysis*

The BPA concentration was determined by high performance liquid chromatography (HPLC) consisting of a reverse-phase column (Pinnacle II C-18, 5 μm 250 × 4.6 mm), a high-pressure pump (Spectrasystem P4000), an autosampler (Spectrasystem AS3000) and a UV detector (Spectrasystem UV6000LP). A mobile phase containing acetonitrile and water at 70:30% was used and a detection wavelength of 278 nm was applied. The retention time of the BPA peak under these conditions was recorded as 4.32 min. The total organic carbon (TOC) concentration was determined using a TOC analyzer (Shimadzu 5000A) equipped with an autosampler (ASI-5000A).

3. Results and discussion

3.1. *Characteristics of TiO_2/ITO and Au–TiO_2/ITO films*

During the photoreduction reaction with the TiO_2 suspension, it was observed that the color of TiO_2 particles in the suspension gradually changed from white to purple during illumination. It was noted that the intensity of the purple colour of the Au–TiO_2 powder produced from the photo-reduction increased with the Au content.

The TiO_2/ITO and Au–TiO_2/ITO films prepared as described earlier were first examined by XRD and the XRD pattern of different Au–TiO_2/ITO films are shown in Figure 3. The XRD results showed that both anatase and rutile were present in the Au–TiO_2/ITO films. In addition, the crystalline Au can only be found in the Au–TiO_2/ITO films with a Au content higher than 1.5% as a broad peak at around $2\theta = 44°$, according to Watanabe and Kozuka [36].

The TiO_2/ITO and Au–TiO_2/ITO films were then analyzed by XPS and the analytical results are shown in Figure 4. The XPS of the TiO_2/ITO film (Figure 4(a)) showed the main peaks of O 1s, Ti 2p, C 1s, Ti 3s, and Ti 3p at 532, 460, 284, 66, and 42 eV, respectively, while the XPS of Au–TiO_2/ITO film (Figure 4(b)) showed an extra peak of Au 4f at 84 eV. This Au 4f peak confirmed the existence of the Au element in the Au–TiO_2/ITO film and the C 1s peak resulted from the adsorption of

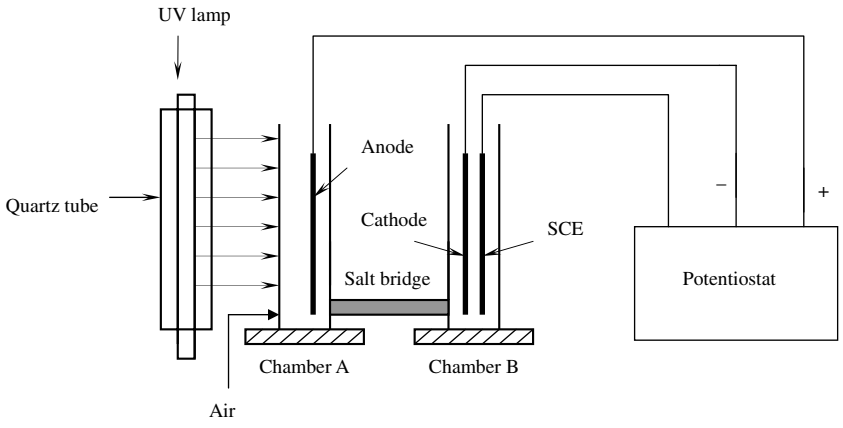

Fig. 2. Schematic diagram of PC and PEC photoreactor systems.

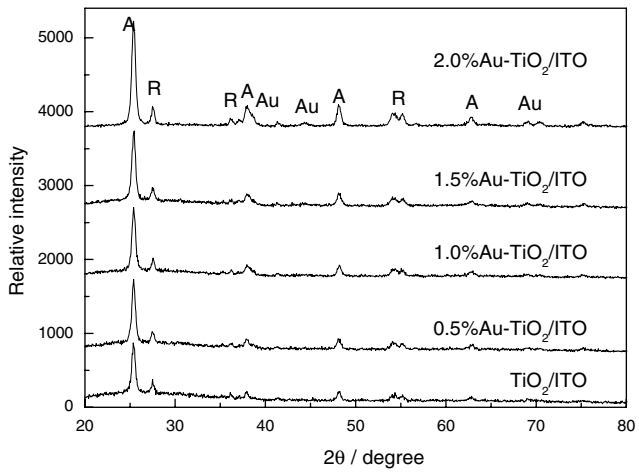

Fig. 3. XRD pattern of TiO_2/ITO and Au–TiO_2/ITO films.

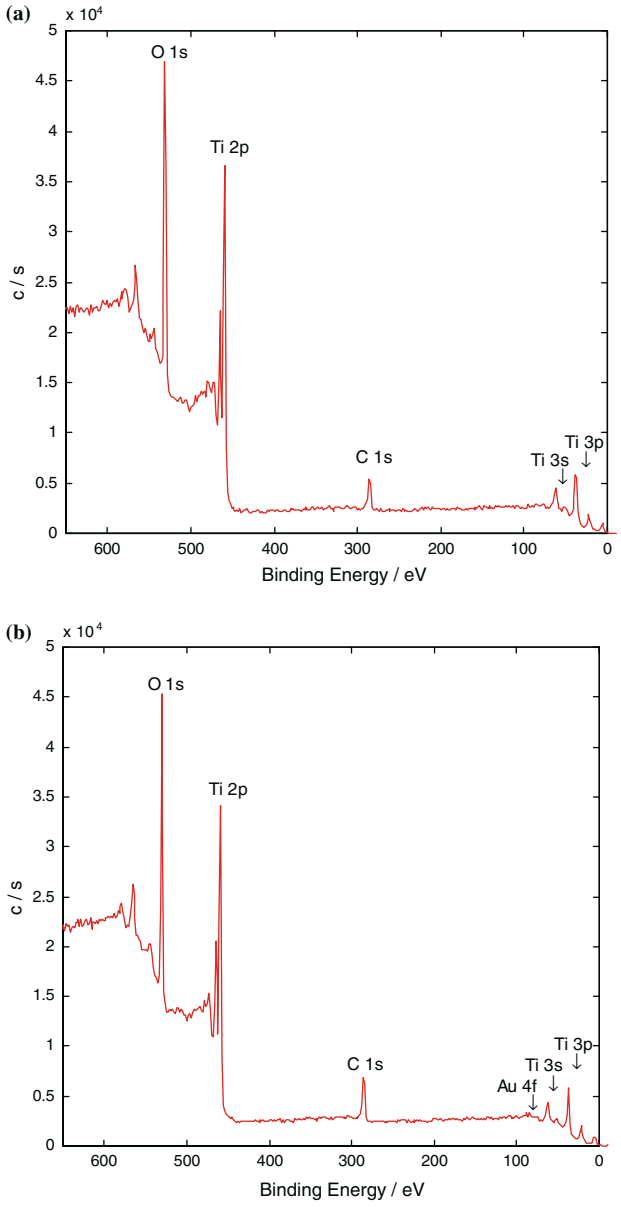

Fig. 4. XPS spectra of (a) TiO_2/ITO film and (b) Au–TiO_2/ITO film.

carbon from the atmosphere by the catalyst films. To study the chemical states of the Au element, the Au–TiO_2/ITO film was further analyzed with a high-resolution scan in the region of the Au 4f orbital and its XPS profiles are shown in Figure 5. Two specific peaks corresponding to binding energies of 82.86 and 86.61 eV were found, representing Au $4f_{7/2}$ and Au $4f_{5/2}$ electrons, respectively. The Au $4f_{7/2}$ and Au $4f_{5/2}$ peaks were fitted using the Multipak 6.0A software and the XPS of Au $4f_{7/2}$ showed that the fitted peak at 82.42 eV could be attributed to Au(0), while the peaks at the higher binding energies of 83.06 and 83.72 eV corresponded to the Au(I) and Au(III), respectively. The XPS of Au $4f_{5/2}$ showed that the peaks at 85.90, 86.60, and 87.30 eV corresponded to the Au(0), Au(I), and Au(III), respectively, according to literatures [18, 37, 38]. These XPS results indicated that the gold ions in the photo-reduction reaction were mainly reduced to Au(0), and with minor portions of Au(I) and Au(III). It is useful to note that some studies have reported that the coexistence of Au(0), Au(I), and Au(III) species at the TiO_2 interface may be beneficial for Au–TiO_2 catalysts bettering terms of greater photocatalytic activity [16–18].

The TiO_2/ITO and Au–TiO_2/ITO films were examined by SEM and their images are presented in Figure 6. It can be seen clearly that both the TiO_2/ITO and Au–TiO_2/ITO films had a porous surface, but the surface of TiO_2/ITO film seemed more porous than the Au–TiO_2/ITO film. It can also be estimated that the TiO_2/ITO film had an average particulate size of around 50 nm, which is bigger than the original size of around 30 nm as P25 TiO_2 powder. Compared to the TiO_2/ITO film, the particulates on the Au–TiO_2/ITO film were more uniformly distributed and were smaller in size. However, these SEM results did not provide clear information about the size distribution of Au deposits in the Au–TiO_2 particulates and high-resolution SEM

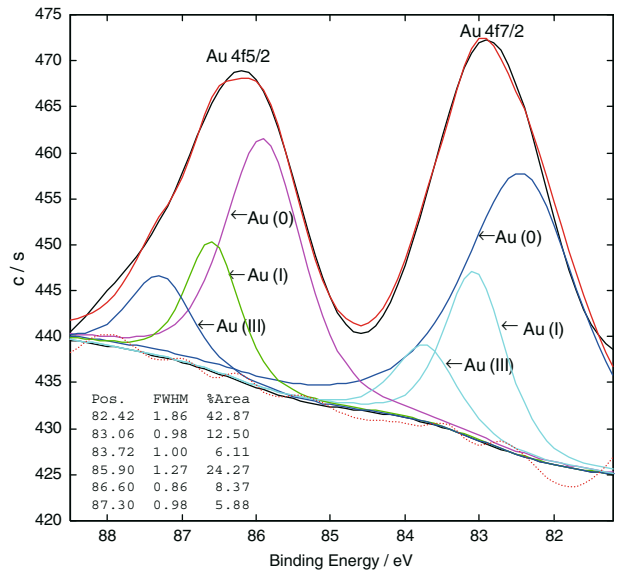

Fig. 5. XPS Au 4*f* spectra of 1.1%Au–TiO_2/ITO film.

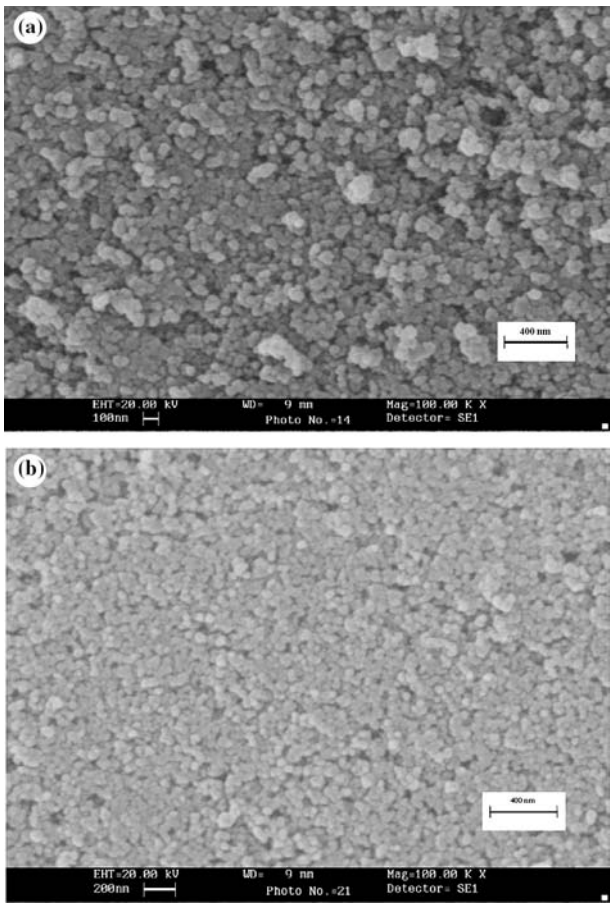

Fig. 6. SEM images of (a) TiO_2/ITO film and (b) 1.1%Au–TiO_2/ITO film.

studies may be necessary to further determine the size distribution.

To determine the optical properties, the TiO_2/ITO and Au–TiO_2/ITO films were also analyzed by UV–VIS absorption spectrometry in the wavelength range of 300–800 nm and the absorption spectra of TiO_2/ITO and Au–TiO_2/ITO films are shown in Figure 7. The absorption spectra results showed that all the Au–TiO_2/ITO films had better optical absorption generally in the whole range than the TiO_2/ITO film, and where the absorption increased significantly with the amount of Au. Moreover, a new significant absorption peak occurred in the region of 500–650 nm, which was attributed to the deposited Au on the surface of the TiO_2 film. The results clearly demonstrated that the Au–TiO_2/ITO films had a significant increase of absorbance in the visible region between 500–600 nm due to Au deposition. It is believed that the enhancement of light absorbance is an essential condition to conduct photocatalytic reactions under visible light irradiation.

3.2. *Photocatalytic activity of TiO_2/ITO and Au–TiO_2/ITO films*

The photocatalytic activity of the TiO_2/ITO and Au–TiO_2/ITO films was evaluated by determining the

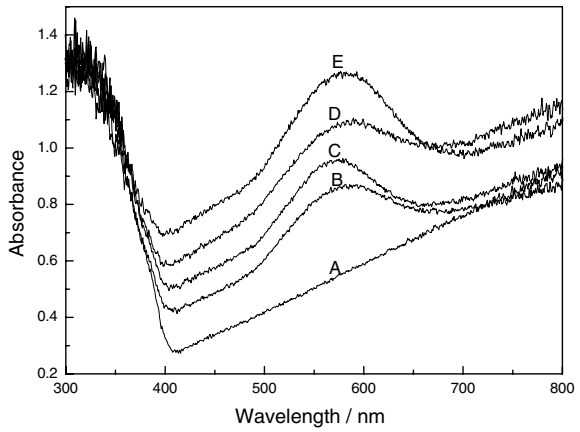

Fig. 7. UV–VIS absorption spectra of (A) TiO_2/ITO; (B) 0.63%-Au–TiO_2/ITO; (C) 1.1% Au–TiO_2/ITO; (D) 1.57% Au–TiO_2/ITO and (E) 2.07%Au–TiO_2/ITO.

degradation of BPA in aqueous solution. Two sets of PC and PEC oxidation tests were carried out with the BPA solution using the TiO_2/ITO and Au–TiO_2/ITO films. All of these tests were carried out with an initial BPA concentration of 16 mg l^{-1} and duration of 50 min, and the experimental results are shown in Figure 8. It can be seen that the degree of BPA degradation varied with the content of Au deposited on the TiO_2. In the PC reaction, the efficiency of BPA degradation increased with the increase of Au content significantly, since the Au deposits on the TiO_2 served as an electron trapper and reduced the recombination of hole-electron pairs. Above 1% of Au content, the degree of BPA degradation only further increased slightly. This is consistent with previous studies where we reported that Au–TiO_2 powder catalysts with an Au content between 0.5 and 1.0% had the highest photocatalytic activity in a slurry system and that a further increase of Au content from 1.0 to 2.0% had a detrimental effect on photocatalytic activity [16, 17]. In this study, the experimental results showed that the photocatalytic activity of Au–TiO_2/ITO films with a

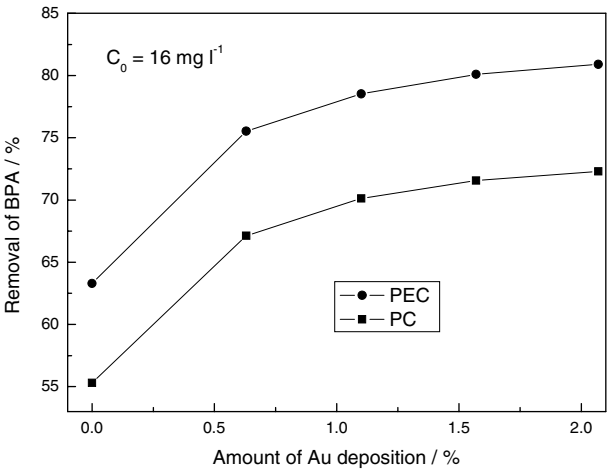

Fig. 8. Variation of BPA degradation with the amount of Au deposition (applied anodic bias +0.8 V vs SCE for PEC process).

Au content of up to 2% achieved an effective performance. These results suggested that the Au–TiO_2/ITO film may have a higher optimal Au content than the Au–TiO_2 powder. For the case of Au–TiO_2 powder suspended in a reacting system, the settling of the Au–TiO_2 particles from the colloid solution would prevent UV-illumination from exciting the Au–TiO_2 catalyst. In contrast, for the Au–TiO_2 film, the Au deposits are uniformly distributed to the entire surface of the film and this makes it possible to avoid the disadvantage with the powder [39]. In the PEC reaction, a similar trend was also found as shown in Figure 8. Furthermore, it was confirmed that the efficiency of BPA degradation in the PEC reaction was considerably higher than that in the PC reaction. Since the 1.1%Au–TiO_2/ITO film achieved a good performance in both the PC and PEC processes, it was selected as a model Au–TiO_2/ITO film and applied in all the following experiments to further study the PEC process.

To investigate the effects of applied bias on the PEC reaction, two sets of BPA degradation experiments were conducted using the TiO_2/ITO and 1.1%Au–TiO_2/ITO films in a 50-min batch reaction, respectively, and applying different anodic bias in the range of 0–8.0 V vs SCE. The experimental results are presented in Figure 9. It can be seen that the degree of BPA degradation increased substantially, and systematically, with the increase in anodic bias. For the TiO_2/ITO film, the degree of BPA degradation increased considerably when the applied anodic bias increased from 0 to 1.5 V vs SCE, and then increased more gradually and in a declining manner up to 8 V vs SCE. These results are in good agreement with the work by Kim and Anderson [13]. For the 1.1%Au–TiO_2/ITO film, the degree of BPA degradation increased substantially when the applied anodic bias changed from 0 to 0.8 V vs SCE and at 0.8 V vs SCE a high degree of BPA degradation of 78.6% was achieved. Thereafter, when the anodic bias was increased from 0.8 to 8 V vs SCE there was only a minimal increase in the extent of BPA degradation. These results indicated that the bias of 0.8 V vs SCE would be an optimal value under the experimental conditions, providing enough potential to the flat band potential to make an effective charge separation by withdrawing electrons to the counter electrode [13]. A blank experiment was also carried out by applying an anodic bias of 0.8 V vs SCE, but without illumination. The experiment demonstrated that the reduction of BPA was insignificant, confirming the absence of any direct oxidation of BPA between the electrodes. Therefore, it may be concluded that the externally-applied anodic bias was able to drive away the accumulated electrons on the Au particles via the external circuit and thus promote the photocatalytic degradation of BPA. Bearing in mind that oxygen evolution at higher voltage would result in the destruction of the catalyst film [31], the anodic bias of 0.8 V vs SCE was consequently applied to the following experiments.

To identify the most effective reactor system, a set of comparative tests was carried out and the experimental results are shown in Figure 10. The results confirmed that the PEC reaction was faster than the PC reaction and the Au–TiO_2/ITO film had a higher photocatalytic activity for the degradation of BPA than TiO_2/ITO film under the experimental conditions. The experimental data were found to fit closely a pseudo-first-order kinetic model and the values of the kinetic constant, k, are listed in Table 1. It can be seen that the reaction rate for the four reactor systems can be ranked from high to low as (D) > (C) > (B) > (A). The PEC reaction using the 1.1% Au–TiO_2/ITO film achieved the highest BPA removal of 99% after 2 h under UV irradiation. During the BPA degradation reaction, the solution TOC was also monitored and the experimental results are shown in Figure 11. The experiments demonstrated that the extent of TOC removal was significantly lower (≈30%) than that of the BPA degradation within the limited reaction period. These results indicated that BPA

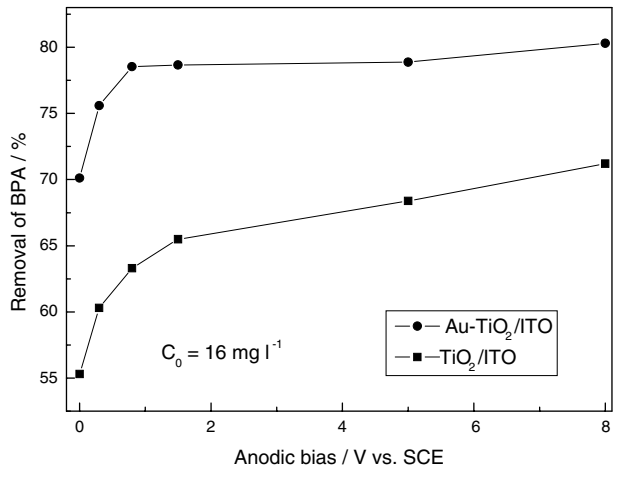

Fig. 9. Variation of BPA degradation with applied anodic bias +0.8 V for TiO_2/ITO and 1.1%Au–TiO_2/ITO film for a set of 50-min reactions.

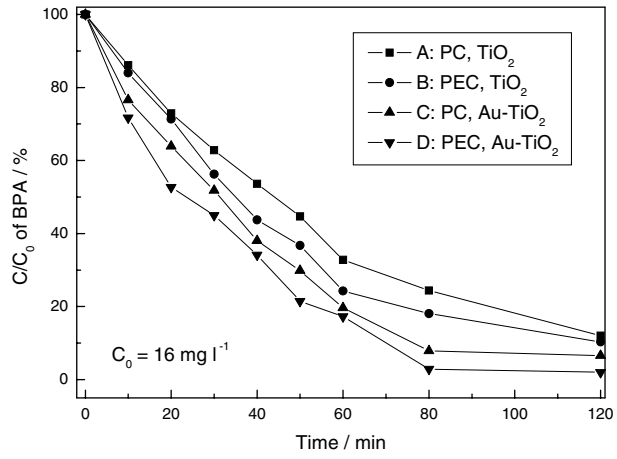

Fig. 10. Comparison of BPA degradation for different reactor systems.

Table 1. The values of the first-order kinetic coefficient, k, for four reactor systems (A–D)

ID	Catalyst	Process	Rate constant k min^{-1}	Correlation coefficient (R)
A	TiO_2/ITO	PC	0.017	0.9919
B	TiO_2/ITO	PEC	0.021	0.9907
C	1.1%Au–TiO_2/ITO	PC	0.025	0.9930
D	1.1%Au–TiO_2/ITO	PEC	0.029	0.9945

was photocatalytically oxidized via a number of intermediates prior to its final product of CO_2, in which some intermediates were further degraded at a lower reaction rate but without complete conversion to CO_2. Overall, it can be seen that the TOC removal in the PEC process using Au–TiO_2/ITO was greater than that either in the PC process using Au–TiO_2/ITO or in the PEC process using TiO_2/ITO.

3.3. *Study of charge separation*

Many researchers have demonstrated that Au nanoparticulates possess a property of electron storage [12, 15–19]. When a semiconductor such as TiO_2 and metal nanoparticulates such as Au are in contact, the photogenerated electrons are transferred from the exited TiO_2 to Au due to a higher Fermi level of Au of approximately $+0.5$ V vs NHE [12] until equilibration. This electron transfer can promote an interfacial charge-transfer process.

To better understand such an electron transfer process, two electrochemical experiments were conducted in an O_2-saturated solution and a N_2-saturated solution, respectively, in which different films were applied and the open circuit photovoltage (V_{oc}) of the electrode under UV illumination was determined by a potentiostat. The experimental results are shown in Figure 12. It can be seen that the V_{oc} of the Au–TiO_2/ITO electrode in the O_2-saturated solution was always lower than that in the N_2-saturated solution. This phenomenon can be explained by the surface-adsorbed O_2 scavenging the photogenerated electrons from the Au–TiO_2 electrode in the O_2-saturated environment, thereby resulting in a lower value of V_{oc}. The results also showed that the V_{oc} of the Au–TiO_2/ITO electrode decreased substantially with the increase of Au content, since the greater quantity of Au deposits on the TiO_2 surface trapped more photogenerated electrons and diminished the electron accumulation in the catalyst. Furthermore, two more experiments were carried out with the N_2-saturated solution using the TiO_2/ITO and Au–TiO_2/ITO electrodes, respectively, and the open circuit voltage was measured with and without illumination. The experimental results are shown in Figure 13. It can be seen that the open circuit voltage of the TiO_2/ITO electrode had no significant reduction after illumination was off, but for the Au–TiO_2/ITO electrode the voltage declined remarkably. Since the experiments were carried out with the N_2-saturated solution, the decay of open circuit voltage results from the mechanism of H_2 evolution instead of O_2 reduction. These experimental results confirmed that H_2 evolution only occurred on the Au–TiO_2/ITO surface, and not on the TiO_2/ITO surface due to the presence of a high overpotential for the evolution of hydrogen at the TiO_2/ITO electrode, although the potential of its conduction band (-0.2 V vs NHE) is sufficient to reduce H^+ [40].

To further study the interfacial charge transfer process in the presence of an external bias, a set of four experiments in the N_2-saturated solution with an electrolyte of 0.05 mol l^{-1} Na_2SO_4 was carried out with and without illumination, in which the photo-anodic current was measured when different potentials were applied in

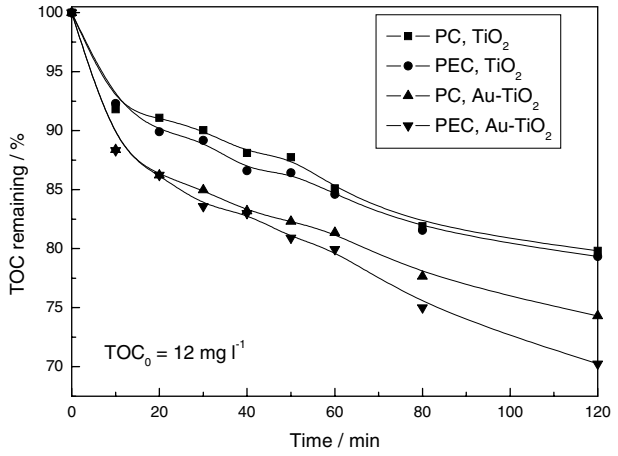

Fig. 11. Comparison of TOC removal in the BPA degradation for different reactor systems.

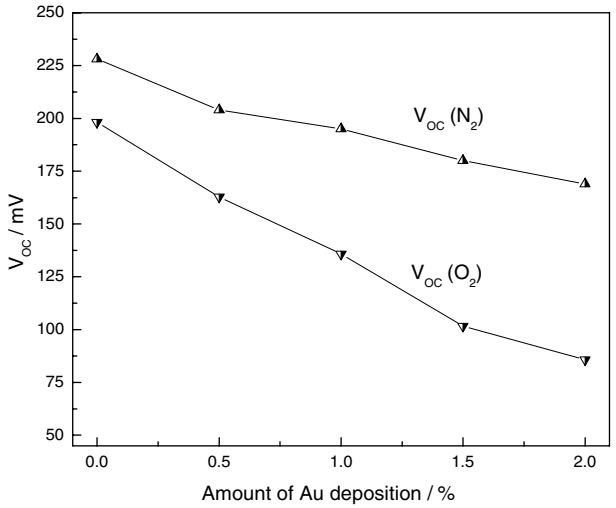

Fig. 12. Open circuit voltage (V_{oc}) of Au–TiO_2/ITO electrode under illumination in the N_2-saturated solution and the O_2-saturated solution.

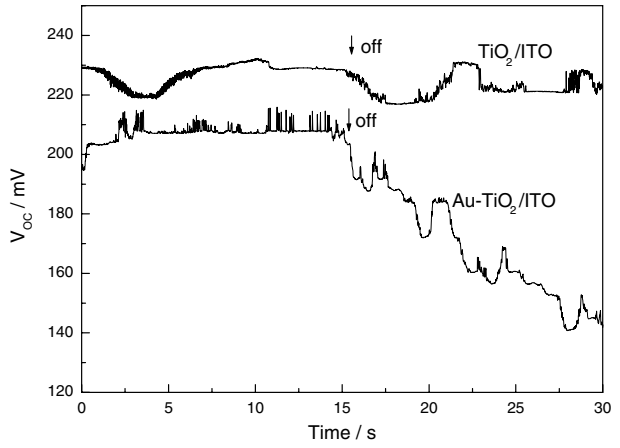

Fig. 13. Decay curves of open circuit voltage (V_{oc}) with and without illumination.

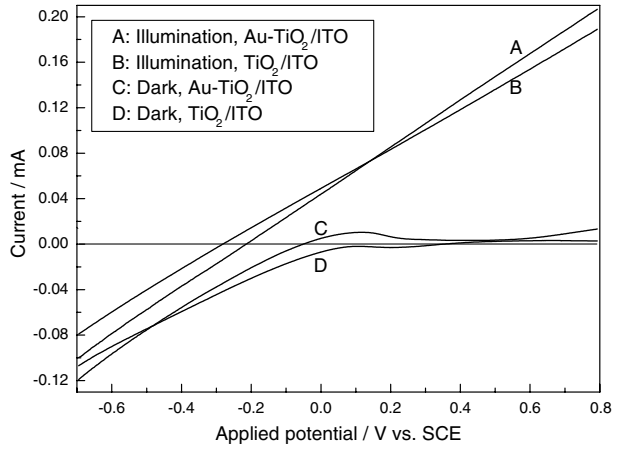

Fig. 14. Dependence of the photocurrent on applied voltage (sweep rate: 20 mV s^{-1}, scan from −0.7 to +0.8 V vs SCE, accuracy: ±10 mV and 0.05 mol l^{-1} Na_2SO_4 as electrolyte) for different reactor conditions.

the range −0.6 to +0.8 V vs SCE. The experimental results are shown in Fig. 14. The results indicated that in dark conditions, only a cathodic current for either Au–TiO_2/ITO or TiO_2/ITO film was observed, in agreement with the results reported by Vinodgopal et al. [23]. Under illumination, both the TiO_2/ITO and Au–TiO_2/ITO electrodes exhibited an additional anodic photocurrent which increased almost linearly with an increase in applied potential. However, the anodic photocurrent of the Au–TiO_2/ITO electrode increased with a measurably higher gradient than that of the TiO_2/ITO electrode. It can be seen that when the applied potential was −0.6 V vs SCE, the cathodic current of the TiO_2/ITO electrode was lower than that of the Au–TiO_2/ITO electrode, and when the applied potential was +0.8 V vs SCE, the anodic current of the TiO_2/ITO electrode was also lower than that of the Au–TiO_2/ITO electrode. A point of equal current for both systems was observed at an applied potential of around +0.1 V vs SCE. These results have shown that the application of an anodic bias to the Au–TiO_2/ITO electrode provided a potential gradient within the film to efficiently force the photogenerated electrons to arrive at the counter electrode [23, 26]. It is evident that the electrons on the Au–TiO_2/ITO electrode were more easily driven away by the same applied potential, whether positive or negative.

In addition, a set of experiments was conducted to monitor the pattern of photocurrent generated on the TiO_2/ITO electrode versus illumination time with the applied potential of +0.8 V vs SCE. Two experiments were carried out in the N_2- and O_2-saturated solutions, respectively, and illumination was switched on and off in a cycle mode. The photocurrent-time profiles are shown in Figure 15. It can be seen clearly that in the O_2-saturated solution, the TiO_2/ITO electrode showed a rapid response of photocurrent upsurge and decline when the illumination was cycled on and off. Such a pattern of curves was maintained throughout the whole experiment of 120 min. These results indicated that the accumulated electrons on the TiO_2/ITO electrode were quickly driven away in the O_2-saturated condition after illumination stopped, which was also reported by Vinodgopal et al. [23]. However, the results also demonstrated a very different variation of photocurrent in the N_2-saturated solution. There was no sharp response of photocurrent on the TiO_2/ITO electrode, when illumination was cycled on and off. This result indicated that the photoelectrons which accumulated on the TiO_2/ITO electrode could not be effectively driven away in the N_2-saturated condition after illumination had stopped. Consequently, two more experiments were carried out using the Au–TiO_2/ITO electrode in both the O_2- and N_2-saturated solutions, respectively, and the photocurrent-time profiles are shown in Figure 16. The response of the Au–TiO_2/ITO electrode demonstrated a similar pattern of photocurrent variation in both the O_2-and N_2-saturated solutions. These results confirmed that the accumulated electrons were effectively transferred by the Au–TiO_2/ITO electrode even in the N_2-saturated solution.

On the basis of the experimental results, it can be concluded that the Au–TiO_2/ITO electrode demon-

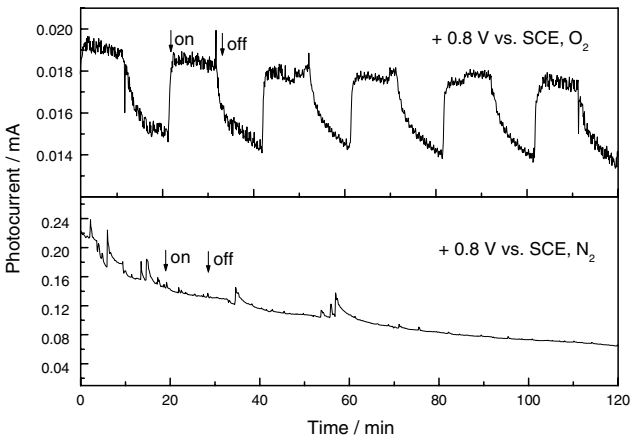

Fig. 15. Photocurrent-time profiles of TiO_2/ITO electrode corresponding to the on-off cycles of illumination.

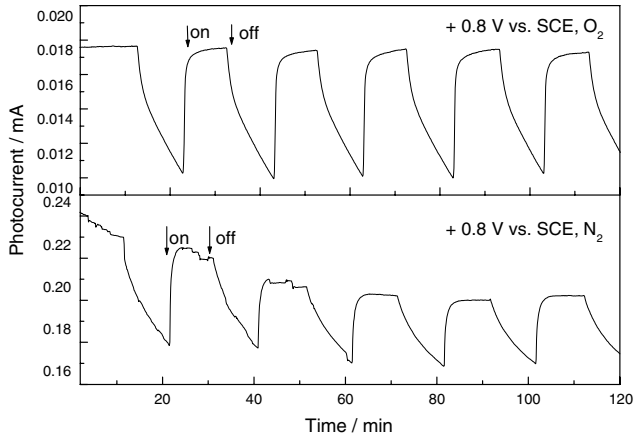

Fig. 16. Photocurrent-time profiles of Au–TiO_2/ITO electrode corresponding to the on–off cycles of illumination.

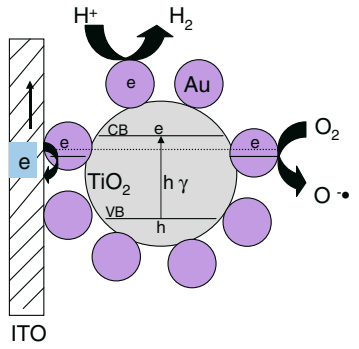

Fig. 17. Scheme of charge separation in an Au–TiO_2/ITO electrode.

strated an effective role in terms of electron transfer in the PEC reaction. The mechanism of the electron transfer in this system is illustrated in Figure 17. It is proposed that the photo-generated electrons on the Au–TiO_2/ITO electrode under illumination in a PEC process can be transferred via three alternative mechanisms: (1) the reaction with O_2 reduction; (2) the reaction with H_2 evolution; and (3) the electron trapping by Au deposits and further transfer out of the electrode through an applied bias. However, it is unclear which reaction is the rate determining step and it is possible that all three mechanisms may work together in an integrated manner.

4. Conclusions

In this study, TiO_2/ITO and Au–TiO_2/ITO films were prepared and fully characterized by different analyses. The photocatalytic activity of the prepared films was evaluated via the oxidative degradation of BPA. The results have demonstrated that the degree of BPA degradation using Au–TiO_2/ITO films was significantly higher than that using the TiO_2/ITO film in both the PC and PEC processes. The enhancement is attributed to the action of Au deposits on the TiO_2 surface, which play a key role by attracting conduction band photoelectrons. In the PEC process, the anodic bias externally applied on the illuminated Au–TiO_2/ITO film can further drive away the accumulated photoelectrons from the metal deposits and promote a process of interfacial charge transfer. It is believed that the use of a Au–TiO_2/ITO photoelectrode as the basis of a PEC process would be an effective treatment technology for removing EDCs from raw waters and wastewaters.

Acknowledgements

The authors wish to acknowledge the financial support of The Hong Kong Polytechnic University (Project No. G-T607) and China National Natural Science Foundation (Project No. 20277046) for this research.

References

1. T. Colborn, *Environ. Toxicol. Chem.* **17** (1998) 1.
2. M. Ahel, T. Conrad and W. Giger, *Environ. Sci. Technol.* **21** (1987) 697.
3. T. Horiguchi, H. Shiraishi, M. Shimizu and M. Morita, *Environ. Pollut.* **95** (1997) 85.
4. S.F. Arnold, D.M. Klotz, B.M. Collins, P.M. Vonier, L.J. Guillette Jr. and J.A. McLachlan, *Science* **272** (1996) 1489.
5. G.G. Ying, B. Williams and R. Kookana, *Environ. Int.* **28** (2002) 215.
6. T. Nakashima, Y. Ohko, D.A. Tryk and A. Fujishima, *J. Photochem. Photobiol. A* **151** (2002) 207.
7. J. Spivack, T.K. Leib and J.H. Lobos, *J. Biol. Chem.* **269** (1994) 7323.
8. M.J. Hemmer, B.L. Hemmer, C.J. Bowman, K.J. Kroll, L.C. Folmar, D. Marcovich, M.D. Hoglund and N.D. Denslow, *Environ. Toxicol. Chem.* **20** (2001) 336.
9. M.R. Hoffmann, S.T. Martin, W.Y. Choi and D.W. Bahnemann, *Chem. Rev.* **95** (1995) 69.
10. A. Fujishima, T.N. Rao and D.A. Tryk, *J. Photochem. Photobiol C* **1** (2000) 1.
11. G. Ceñti, P. Ciambelli, S. Perathoner and P. Russo, *Catal. Today* **75** (2002) 3.
12. N. Chandrasekharan and P.V. Kamat, *J. Phys. Chem. B* **104** (2000) 10851.
13. D.H. Kim and M.A. Anderson, *Environ. Sci. Technol.* **28** (1994) 479.
14. G.R. Bamwenda, S. Tsubota, T. Nakamura and M. Haruta, *J. Photochem. Photobiol. A* **89** (1995) 177.
15. V. Subramanian, E. Wolf and P.V. Kamat, *J. Phys. Chem. B* **105** (2001) 11439.
16. X.Z. Li and F.B. Li, *Environ. Sci. Technol.* **35** (2001) 2381.
17. F.B. Li and X.Z. Li, *Appl. Catal. A* **228** (2002) 15.
18. I.M. Arabatzis, T. Stergiopoulos, D. Andreeva, S. Kitova, S.G. Neophytides and P. Falaras, *J. Catal.* **220** (2003) 127.
19. A. Dawson and P.V. Kamat, *J. Phys. Chem. B* **105** (2001) 960.
20. W. Zhao, C. Chen, X. Li, J. Zhao, H. Hidaka and N. Serpone, *J. Phy. Chem. B* **106** (2002) 5022.
21. X.Z. Li and F.B. Li, *J. Appl. Electrochem.* **32** (2002) 203.
22. H. Selcuk, W. Zaltner, J.J. Sene, M. Bekbolet and M.A. Anderson, *J. Appl. Electrochem.* **34** (2004) 653.
23. K. Vinodgopal, S. Hotchandani and P.V. Kamat, *J. Phys. Chem.* **97** (1993) 9040.
24. J. Rodriguez, M. Gomez, S.E. Lindquest and C.G. Granqvist, *Thin Solid Films* **360** (2000) 250.
25. X.Z. Li, H.L. Liu, P.T. Yue and Y.P. Sun, *Environ. Sci. Technol.* **34** (2000) 4401.

26. M.V.B. Zanoni, J.J. Sene and M.A. Anderson, *J. Photochem. Photobiol. A* **157** (2003) 55.
27. C. He, Y. Xiong, C. Zha, X. Wang and X. Zhu, *J. Chem. Technol. Biotechnol.* **78** (2003) 717.
28. C. He, Y. Xiong and X. Zhu, *Thin Solid Films* **422** (2002) 235.
29. C. He, Y. Xiong, J. Chen, C. Zha and X. Zhu, *J. Photochem. Photobiol. A* **157** (2003) 71.
30. C. He, Y. Xiong and X. Zhu, *Catal. Commun.* **4** (2003) 183.
31. C. He, Y. Xiong and X. Zhu, *J. Eniorn. Sci. Health A* **37** (2002) 1545.
32. A. Sclafani and J.M. Hermann, *J. Photochem. Photobiol. A* **113** (1998) 181.
33. S.R. Howe, L. Borodinsky and R.S. Lyon, *J. Coat. Technol.* **70** (1998) 69.
34. J. Sajiki and J. Yonekubo, *Chemosphere* **51** (2003) 55.
35. D. Arenholt-Bindslev, V. Breinholt, A. Preiss and G. Schmalz, *Clin. Oral Invest.* **3** (1999) 120.
36. A. Watanabe and H. Kozuka, *J. Phys. Chem. B* **107** (2003) 12713.
37. T. Ioannides and X.E. Verykios, *J. Catal.* **161** (1996) 560.
38. NIST X-ray Photoelectron Spectroscopy Database, NIST Standard Reference Database 20, Version 3.4 (Web Version), the National Institute of Standards and Technology (NIST) Technology Services..
39. J. Sheng, L. Shivalingappa, J. Karasawa and T. Fukami, *J. Mater. Sci.* **34** (1999) 6201.
40. K. Rajeshwar, *J. Appl. Electrochem.* **25** (1995) 1067.